SUPPLEMENTAL INFORMATION

SUPPLEMENTAL NOTES

Note I: Osmotic minipumps, delivering either 1.5 µg/day recombinant mouse VEGF-B$_{167}$ protein (rmVEGF-B$_{167}$, a kind gift from Dr. A. Nash (Amrad Corporation, Melbourne, Australia) or saline vehicle, were implanted subcutaneously in WT mice, subjected to myocardial infarction, and the blood plasma levels of mVEGF-B$_{167}$ were measured at 4 days after pump implantation by using a modified version of a previously established home-made ELISA [1]. This mouse VEGF-B$_{167}$ ELISA is more sensitive compared to the human VEGF-B$_{167}$ ELISA, and we therefore chose to analyze the biodistribution of mVEGF-B$_{167}$. Administration of rmVEGF-B$_{167}$ via osmotic minipumps increased the blood plasma levels of mVEGF-B$_{167}$ from below the detection threshold of the ELISA (<0.13 ng/ml) after saline treatment towards 1.5 ± 0.2 ng/ml after rmVEGF-B$_{167}$ therapy (N=4; P<0.05), indicating that our delivery strategy indeed increased the circulating levels of mVEGF-B$_{167}$. We were unable to find increased levels of mVEGF-B$_{167}$ in heart extracts (not shown), likely due to the high endogenous levels of mVEGF-B$_{167}$ in the heart [2].

Note II: Systemic adenoviral VEGF-B$_{167}$ gene delivery is known to transduce hepatocytes that then release the transgene product. Adenoviral vectors encoding hVEGF-B$_{167}$ (Ad.hVEGF-B$_{167}$) or control vectors (Ad.RR5) were injected intravenously at 3x10^9 p.f.u. per mouse, immediately after ligation of the LAD or femoral artery. In mice, treated with a control adenovirus (Ad.RR5) [3], hVEGF-B plasma levels were below the threshold of detection (<0.50 ng/ml). However, after intravenous injection of Ad.hVEGF-B$_{167}$, at the time of LAD ligation, circulating hVEGF-B$_{167}$ levels were as high as 5 ng/ml at 7 days post-MI (N=10; P<0.05). In addition, after ligation of the femoral artery, the circulating levels of hVEGF-B$_{167}$ increased for periods up to 3 weeks (ng/ml plasma: 4.1 ± 0.6, 4.7 ± 0.4, 2.6 ± 0.9, 1.8 ± 0.5 ng/ml at 3, 7, 14 and 21 days post-ligation; N=8; P<0.05 *versus* undetectable levels after Ad.RR5 at all days), while by 28 days post-ligation, hVEGF-B$_{167}$ levels reached the detection threshold of the assay.

Note III: A delayed effect of Ad.hVEGF-B$_{167}$ gene transfer on revascularization of ischemic limbs was excluded since, also at 28 days after ischemia, VEGF-B$_{167}$ therapy failed to improve total limb perfusion, angiogenesis in the gastrocnemius muscle (capillary-to-myocyte ratio: 1.71 ± 0.07 after Ad.RR5 *versus* 1.77 ± 0.14 after Ad.hVEGF-B$_{167}$; N=5;

P=NS), and size and number of collateral vessels in the adductor muscle (lumen area in μm^2: main collateral, 2nd and 3rd collateral branch: 2,040 ± 470, 785 ± 54 and 92 ± 14 after Ad.RR5 *versus* 2,390 ± 530, 678 ± 125 and 97 ± 16 after Ad.hVEGF-B$_{167}$; number of collateral side branches per mm^2, 2nd and 3rd collateral branch: 3 ± 0.4 and 12 ± 2.4 after Ad.RR5 *versus* 3 ± 0.4 and 8 ± 0.9 after Ad.hVEGF-B$_{167}$; total perfusion area in $\mu m^2/mm^2$: 3,020 ± 190 after Ad.RR5 *versus* 2,940 ± 620 after Ad.hVEGF-B$_{167}$; N=5; P=NS).

Note IV: To selectively analyze the effects on collateral growth, we locally delivered VEGF-B$_{167}$ in the adductor muscle via *in vivo* electroporation of a plasmid expressing murine VEGF-B$_{167}$ (pmVEGF-B$_{167}$) – a technique enabling stable overexpression of a transgene for several weeks starting from 1 day after electroporation [4, 5] – we achieved a 6-fold increase in the expression levels of mVEGF-B in the adductor muscle at 8 days after electroporation (pg/mg protein: 651 ± 122 after pmVEGF-B$_{167}$ *versus* 119 ± 15 after empty plasmid; N=6; P<0.05). One day after electroporation (i.e. when the transgene is already expressed [5]), mice were subjected to limb ischemia and sacrificed 7 days later to analyze collateral growth in the adductor muscle. Compared to control, pmVEGF-B$_{167}$ electroporation failed to increase the number or size of the pre-existing collateral vessels (Table 1), indicating that VEGF-B$_{167}$ therapy did not stimulate collateral vessel growth in the limb. Laser Doppler analysis also failed to show better perfusion of the ischemic limbs after local pmVEGF-B$_{167}$ electroporation (Table 1).

SUPPLEMENTAL TABLES

Table I: Negligible role of VEGF-B in pulmonary vessel remodeling after hypoxia

	WT mice		VEGF-B$^{-/-}$ mice	
	normoxia	hypoxia	Normoxia	hypoxia
Vessel remodeling (per 10^3 alveoli)				
Non-muscularized vessels	6.8 ± 0.4	3.4 ± 0.01*	7.6 ± 0.4	3.8 ± 0.3*
Partially-muscularized vessels	3.0 ± 0.1	4.5 ± 0.3*	3.8 ± 0.4	4.4 ± 0.4
Muscularized vessels	1.0 ± 0.3	4.6 ± 0.9*	1.1 ± 0.2	5.2 ± 0.2*
SMA$^-$ vessels	9.3 ± 0.7	4.9 ± 0.1*	10.3 ± 0.3	4.6 ± 1.2*
SMA$^\pm$ vessels	1.5 ± 0.2	4.3 ± 0.8*	2.6 ± 0.3	4.5 ± 0.2*
SMA$^+$ vessels	0.1 ± 0.1	2.7 ± 0.6*	0.1 ± 0.1	2.0 ± 0.6*
Arterial media thickness (µm)	1.53 ± 0.1	2.01 ± 0.08*	1.50 ± 0.07	2.15 ± 0.12*
RV hypertrophy [RV/(LV+S)]	0.20 ± 0.01	0.26 ± 0.01*	0.20 ± 0.02	0.25 ± 0.01*
Hematocrit (%)	32 ± 2.5	43 ± 1.4*	35 ± 0.7	45 ± 2.6*

Pulmonary vessel remodeling, induced by chronic exposure to hypoxia and resulting in pulmonary hypertension, was examined in WT and VEGF-B$^{-/-}$ mice. The density of pulmonary vessels was determined, while discriminating between non-muscularized vessels (with only an internal elastic membrane (IEL)), partially-muscularized vessels (IEL and partial external elastic membrane (EEL)) and muscularized vessels (complete IEL and EEL). To evaluate right ventricle (RV) hypertrophy, the dry weight of the RV was measured and divided by the total dry weight of the left ventricle plus septum (LV+S). Values are means ± SEM. * P<0.05 *versus* normoxia; P=NS for WT mice *versus* VEGF-B$^{-/-}$ mice.

SUPPLEMENTAL FIGURE LEGENDS

Figure I: As an alternative method to deliver VEGF-B to cardiomyocytes, we implanted in the myocardial wall of the infarct border, mouse myoblasts, transduced *ex vivo* with a retrovirus, to constitutively produce mouse VEGF-B$_{167}$, since a similar strategy using VEGF-A-expressing myoblasts was previously shown to stimulate vessel growth in muscle [6-8]. *A,B,* Immunofluorescent staining for VEGF-B (green) confirmed the absence of VEGF-B in control myoblasts expressing only LacZ (*A*) and production of mVEGF-B$_{167}$ in myoblasts expressing both VEGF-B and LacZ (*B*). Nuclei are counterstained with Dapi (blue). The production of mVEGF-B$_{167}$ by engineered myoblasts in vivo was further confirmed by determining mVEGF-B expression levels in cell lysates and muscle extracts. Indeed, myoblasts, transduced with a retrovirus encoding mVEGF-B$_{167}$, secreted 26 ± 2 ng/10^6 cells/24h of VEGF-B, while control LacZ-expressing myoblasts failed to express detectable amounts of VEGF-B. At 3 days after implantation of myoblasts into the gastrocnemius muscle, increased amounts of VEGF-B protein were found in the muscles implanted with the VEGF-B$_{167}$-expressing myoblasts (299 ± 67 pg/mg protein *versus* 22 ± 2 pg/mg protein in control muscles; *N*=6; *P*<0.05). Further in vitro experiments revealed that the secreted VEGF-B protein was bio-active (not shown). *C,D,* Double immunofluorescent staining for ß-galactosidase (site of myoblast engraftment) and CD31 (blood vessels) in the ischemic myocardium revealed no signs of vessel growth around the implantation site of control myoblasts (*C*), but a robust angiogenic induction around the site of VEGF-B$_{167}$-expressing myoblast implantation (*D*). Thus, intramyocardial implantation of VEGF-B$_{167}$-expressing myoblasts enhanced vessel growth in the ischemic myocardium at 28 days post-MI, while control LacZ$^+$ myoblasts failed to promote angiogenesis. Scale bars: 50 µm.

Figure II: We showed previously that adenoviral gene transfer of PlGF into the skin of ears enlarged pre-existing vessels with subsequent stabilization by acquisition of a pericyte coat [9]. We therefore injected adenoviruses, expressing hVEGF-B$_{167}$ (Ad.hVEGF-B$_{167}$), hVEGF-B$_{186}$ (Ad.hVEGF-B$_{186}$) or mPlGF-2 (Ad.mPlGF) intradermally into the ear skin. *A-I,* Ears were whole-mount immunostained for CD31 (endothelial cells; brown) in panels *A,D,G,* for CD31 (green) and SMA (smooth muscle cells; red) in panels *B,E,H*, and for F4/80 (macrophages, green) and SMA (red) in panels *C,F,I*. As expected, gene transfer of mPlGF-2 increased the density, tortuosity and size of pre-existing vessels, and

stimulated their coverage by mural cells (*A,B*). In contrast, Ad.hVEGF-B$_{167}$ or Ad.hVEGF-B$_{186}$ gene transfer minimally enlarged the pre-existing vessels without increase in number, tortuosity or mural cell coverage (*D,E,G,H*). Consistent herewith, we found that many F4/80+ macrophages had infiltrated after Ad.mPlGF gene transfer, while only few macrophages were present after Ad.hVEGF-B$_{167}$ or Ad.hVEGF-B$_{186}$ gene transfer (*C,F,I*). A control virus (Ad.CMV) failed to affect any of these parameters (not shown). Scale bars: 100 μm in panels *A,B,D,E,G,H* and 50 μm in *C,F,I*.

Figure III: *A-D,* To further analyze the effects of VEGF-B on vessel remodeling and recruitment of mural cells, we examined in VEGF-B$^{-/-}$ mice the remodeling of pulmonary vessels in response to chronic hypoxia [10]. Hart's elastin staining revealed no genotypic differences between WT and VEGF-B$^{-/-}$ mice in pulmonary vessel structure in normoxia (*A,B*; see also Table S1). In WT mice, continuous hypoxic conditions for 4 weeks increased the number of thick-walled muscularized vessels by ~4.6-fold (*C*; Table S1). A comparable 4.7-fold increase in the number of thick-walled muscularized vessels was observed in VEGF-B$^{-/-}$ mice (*D*; Table S1), suggesting that loss of VEGF-B did not impair mural cell recruitment. Similar results were obtained when hypoxic vessel remodeling was analyzed by immunostaining for SMA (Table S1). Consistent herewith, no genotypic differences were observed in the development of right ventricle (RV) hypertrophy, which normally is caused by pulmonary hypertension (Table S1). Compared to WT mice, VEGF-B$^{-/-}$ mice were as sensitive to chronic hypoxia, as evidenced by the similar increase in hematocrit levels (Table S1). The lack of an effect of VEGF-B on pulmonary hypertension is consistent with earlier findings by Louzier *et al.* [11]. *E,F,* To further analyze the effects of VEGF-B on angiogenesis, we studied in VEGF-B$^{-/-}$ mice retinal neovascularization in response to ischemia, using an established model [10]. Neovascularization of the ischemic retina, analyzed by H&E staining on cross-sections, was comparable in WT (*E*) and VEGF-B$^{-/-}$ mice (*F*; arrows indicate neovessels). Indeed, compared to WT mice, loss of VEGF-B failed to reduce the number of endothelial cells, forming new intravitreal vessel sprouts (per retinal cross-section: 102 ± 13 in WT mice *versus* 118 ± 10 in VEGF-B$^{-/-}$ mice; *N*=5; *P*=NS) or the number of neovascular tufts (per retinal cross-section: 42 ± 4 in WT mice *versus* 50 ± 8 in VEGF-B$^{-/-}$ mice; *N*=5; *P*=NS; Figure S3*E,F*). These findings are consistent with findings by Reichelt *et al.* [12]. Scale bars: 50 μm in panels *E,F* and 25 μm in panels *A-D.*

Figure IV: *A-D,* At 7 days after ligation, laser Doppler perfusion analysis on ischemic limbs also failed to show any genotypic differences (*A,B*; see also Table 1). Ischemic limb perfusion was also measured in mice lacking both VEGF-B and PlGF – the rationale for this experiment being that limb perfusion was reduced in PlGF$^{-/-}$ mice [10] and that, possibly, the consequences of VEGF-B deficiency might be more apparent when limb revascularization was already impaired by prior loss of PlGF. However, at 7 days after ischemia, laser Doppler imaging revealed that, compared to WT or VEGF-B$^{-/-}$ mice (Table 1; *P*<0.05), limb perfusion was comparably reduced in mice lacking PlGF alone or in mice lacking both VEGF-B and PlGF (*C,D*; % perfusion of non-ligated limb: 47 ± 5% in PlGF$^{-/-}$ mice *versus* 55 ± 9% in VEGF-B$^{-/-}$:PlGF$^{-/-}$ mice; *N*=5; *P*=NS). Please note the color scale: from blue (low perfusion) to red (high perfusion). *E,F,* H&E staining of transverse sections through the adductor muscles revealed a comparable size of the main collateral vessel in WT (*E*) and VEGF-B$^{-/-}$ mice (*F*). *G-I,* Morphometric analysis revealed a similar amount of F4/80^{+} macrophages around the collaterals in WT and VEGF-B$^{-/-}$ adductor muscles (*G*), as also illustrated by microscopic pictures (*H,I*). In addition, VEGF-B failed to stimulate the production by cultured macrophages of TNF-alpha, previously implicated in collateral growth [9] (data not shown). Please note that the black staining inside the vessels results from bismuth-gelatin filling of the vessels, which enables a better macroscopic visualization of the collaterals. Scale bars: 50 µm.

SUPPLEMENTAL METHODS

Animal models

Myocardial ischemia model: Myocardial ischemia was induced by ligation of the left anterior descending (LAD) coronary artery in female mice as described [3, 9]. Seven days after LAD ligation, hearts were harvested, sectioned and analysed for vessel densities and/or macrophage infiltration in the infarct area and border zone.

Mouse skin wound model: A standardized 15 mm full-thickness skin incision was made on the back of mice, taking care not to damage the underlying muscle, as described [10]. Wound healing was quantified by daily measuring the width and the length of the wound. Analysis of vessel densities and inflammation was performed in skin sections, harvested 5 days after wounding.

Mouse ear skin assay: Mouse ears, injected with the PlGF or VEGF-B adenoviral vectors, were dissected, fixed in 1% phosphate buffered paraformaldehyde and whole-mount immunostained for endothelial cells, smooth muscle cells and macrophages using fluorescently conjugated secondary antibodies (Alexa 488 or 546, Molecular Probes).

Mouse ischemic retinopathy model: Mice at postnatal day 7 were exposed to hyperbaric (80%) oxygen for 5 days, as described [10]. After returning to normoxia for another 5 days, the eyes were harvested, fixed in 1% paraformaldehyde, paraffin embedded and sectioned. After H&E staining, the number of endothelial cells and vascular tufts in the vitreous cavity were counted, as described [10, 13].

Pulmonary vascular remodeling: Eight-weeks old male mice were placed in a chamber under normobaric hypoxia (10% O_2) or in normal air (21% O_2; control) as described [14]. After 4 weeks, the right ventricular (RV) wall was dissected from the left ventricle (LV) and septum (S), and dried at 55°C before weighing. Alternatively, lungs were perfusion-fixed, dissected and sectioned as described [14]. Pulmonary vascular remodeling was assessed by counting the number of non-muscularized (only IEL), partially muscularized (IEL plus incomplete EEL) and fully muscularized (IEL and complete EEL) peripheral vessels (located distal to the bronchi) per 10^3 alveoli, as described [14].

Ischemic hindlimb model: In male mice, the right femoral artery and vein (proximal to the popliteal artery) and the cutaneous vessels branching from the caudal femoral artery side branch were ligated, avoiding damage of the femorale nerve [9]. Seven days after ligation, functional perfusion measurements of the total limb were performed using a Lisca PIM II camera (Gambro). Perfusion, averaged over 3 images per mouse in the total hindlimb, was expressed as a ratio of right (ischemic) to left (normal) limb. Limb motor

function was determined via treadmill running exercise (Simplex II, Columbus Instruments), after a one-day conditioning training session [15]. The test protocol included a graded exercise test at constant inclination of 10 degrees with increases in belt speed of 2 m/min every 5 minutes. Exhaustion was defined as failure to abandon the shock grid within 15 seconds. After training, the femoral artery was occluded, and at 7 days later, mice were re-tested on the treadmill. Recovery of function was expressed as a ratio to the baseline exercise time. For histology, the gastrocnemius and adductor muscles were harvested at 7 or 28 days after femoral artery ligation. Vessel densities in the regenerating gastrocnemius muscle were determined morphometrically by analyzing the capillary-to-myocyte ratio. Remodeling of collateral vessels and macrophage recruitment in the upper hindlimb were analyzed as described [9]. In brief, collateral side branches were categorized as smaller or larger than 300 μm^2. Total perfusion area was calculated using the total sum of the side branch luminal areas.

Transplantation of VEGF-B$_{167}$-expressing myoblasts: A MFG retrovirus encoding mouse VEGF-B$_{167}$ cDNA, generated as described [6], was used to transduce LacZ-expressing myoblasts. LacZ-expressing myoblasts were used for transplantation to visualize the engrafted cells. Specific expression of the VEGF-B gene was verified by immunofluorescent staining of myoblasts using antibody, recognizing mouse VEGF-B$_{167}$ (R&D Systems). The amount of gene product, secreted by the VEGF-B producing myoblasts *in vitro*, was quantified by ELISA. The biological activity of medium conditioned by VEGF-B producing myoblasts was compared to medium of VEGF-A expressing cells or control myoblasts, using a HUVEC proliferation assay (Cell Titer Aqueous One Solution Assay, Promega). Myoblasts, co-expressing VEGF-B$_{167}$ and LacZ or control LacZ-myoblasts, were injected into the anterior tibial muscle ($5x10^5$ cells/injection) in normal conditions or immediately after femoral artery ligation and transection in adult male SCID mice, as described [8, 16]. At 28 days following surgery, tibialis and myocardial muscles were harvested and double labeled for endothelial cells and muscle fibers expressing the LacZ reporter gene, using a polyclonal rabbit antibody to LacZ (Eppendorf 5-Prime). Capillaries and muscle fibers were counted and expressed as capillary-to-muscle fiber ratio. Myoblasts were also injected in the infarct border zone ($5x10^5$ cells/injection) of female SCID mice, immediately after LAD ligation, and hearts were harvested for histology at 28 days post-MI.

Histology, immunohistochemistry and morphometric analyses

All tissues were fixed in 1% phosphate buffered paraformaldehyde and embedded in paraffin. Serial parasagittal (hearts) or transverse (skin, retina, lung, limb muscle) sections were cut at 8 µm thickness and stained for H&E or Hart's elastin. Immunostainings were performed using primary antibodies for endothelial cells (rabbit anti-thrombomodulin (TM), gift from Dr. R.W. Jackman, Boston, MA; rat anti-CD31, Becton Dickinson), smooth muscle cells (mouse anti-smooth muscle alpha-actin (SMA), Sigma), macrophages (rat anti-Mac3 and rat anti-F4/80, both Becton Dickinson), and ß-Gal (rabbit anti- ß-Gal, Cappel). Following primary antibody incubation, sections were incubated with peroxidase-labeled IgGs (Dako), followed by amplification with the proper tyramide signal amplification systems (Perkin Elmer, Life Sciences). Morphometric analyses of the vessel densities and macrophage positive areas in the ischemic, granulation or wound border tissues were performed using a Zeiss Axioplan microscope with KS300 image analysis software.

Production and administration of VEGF-B protein, plasmid and adenovirus

The recombinant human VEGF-B167 (rhVEGF- B167) protein was obtained from Amrad Corporation (gift from Dr. A. Nash), and its activity was tested using the Ba/F3 pre-B cell viability assay as described [17] (data not shown). Continuous delivery of 1.5 µg/mouse/day rhVEGF-B167 protein was achieved by subcutaneously implanting osmotic minipumps (Alzet, type 2001), as described [3].

Adenoviruses were constructed by cloning the murine PlGF-2, or the human VEGF-B_{167} or VEGF-B_{186} cDNA into the pACCMVpLpA plasmid, using previously published methods [3, 9]. RNA analysis and immunoblotting of extracts and conditioned medium of cells, transduced with the respective adenovirus, revealed that the transduced cells produced murine PlGF-2, hVEGF-B_{167} or hVEGF-B_{186} protein (not shown). For the ear assays, 1×10^9 pfu adenovirus (Ad.mPlGF, Ad.hVEGF-B_{167}, Ad.hVEGF-B_{186} or control Ad.CMV) was injected intradermally in the ears of female NMRInu/nu mice. In the ischemic hind limb model, 3×10^9 pfu adenovirus (Ad.hVEGF-B_{167} or control Ad.RR5) was intravenously injected in the tail vein of male C57BL/6 mice, immediately after ligation of the femoral artery.

A plasmid expressing murine VEGF-B_{167} (pcDNA3.mVEGF-B_{167}) or an empty pcDNA3 plasmid was administered via muscle electroporation as described [4, 5]. Briefly, one day before ligation of the femoral artery, 15 µg of expression plasmid, encoding

mVEGF-B$_{167}$, or 15 µg empty plasmid (both at 1mg/ml in 0.9% NaCl) was injected into the adductor muscle (total volume of 15 µl over 3 injection sites) using a Hamilton syringe, and electrotransfer (five electric pulses of 100V with a fixed pulse duration of 20 ms and an interval of 200 ms; Electro Square Porator ECM 830, BTX, Harvard Bioscience), with Tweezertrode 520 electrodes (BTX, Harvard Bioscience) was performed.
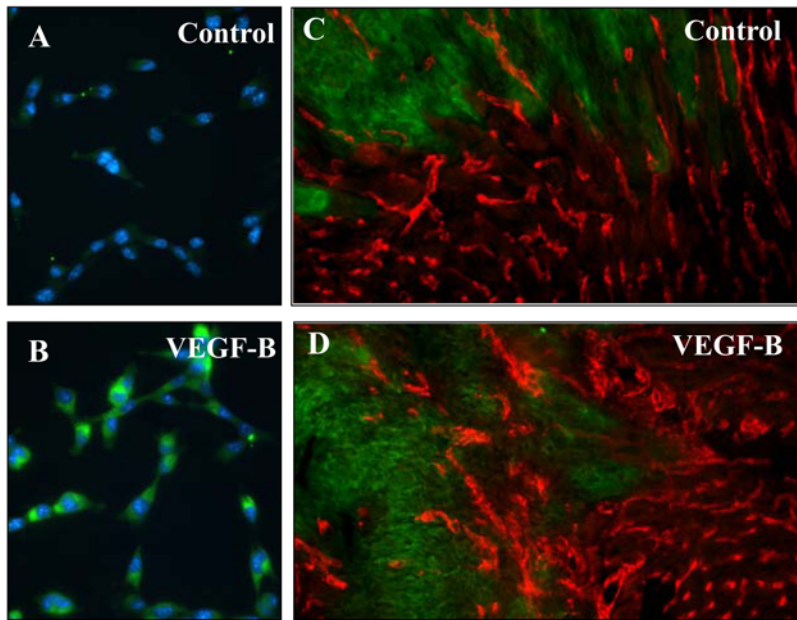
RT-PCR for Flt-1 and ELISA for human and mouse VEGF-B

Quantitative real-time RT-PCR and protein extraction were performed as described [10]. For determining mouse VEGF-B$_{167}$ levels a modified version of a previously established ELISA [1] was used. Plates were coated with a monoclonal antibody to murine VEGF-B (#MAB751, R&D Systems) and mrVEGF-B$_{167}$ (gift from Dr. A. Nash) was used as standard. Human VEGF-B$_{167}$ plasma levels were determined with a home-made ELISA using antibodies (#MAB3372 as capture antibody and #AF751 as detection antibody) and rhVEGF-B$_{167}$ (#751-VE-025) from R&D Systems.
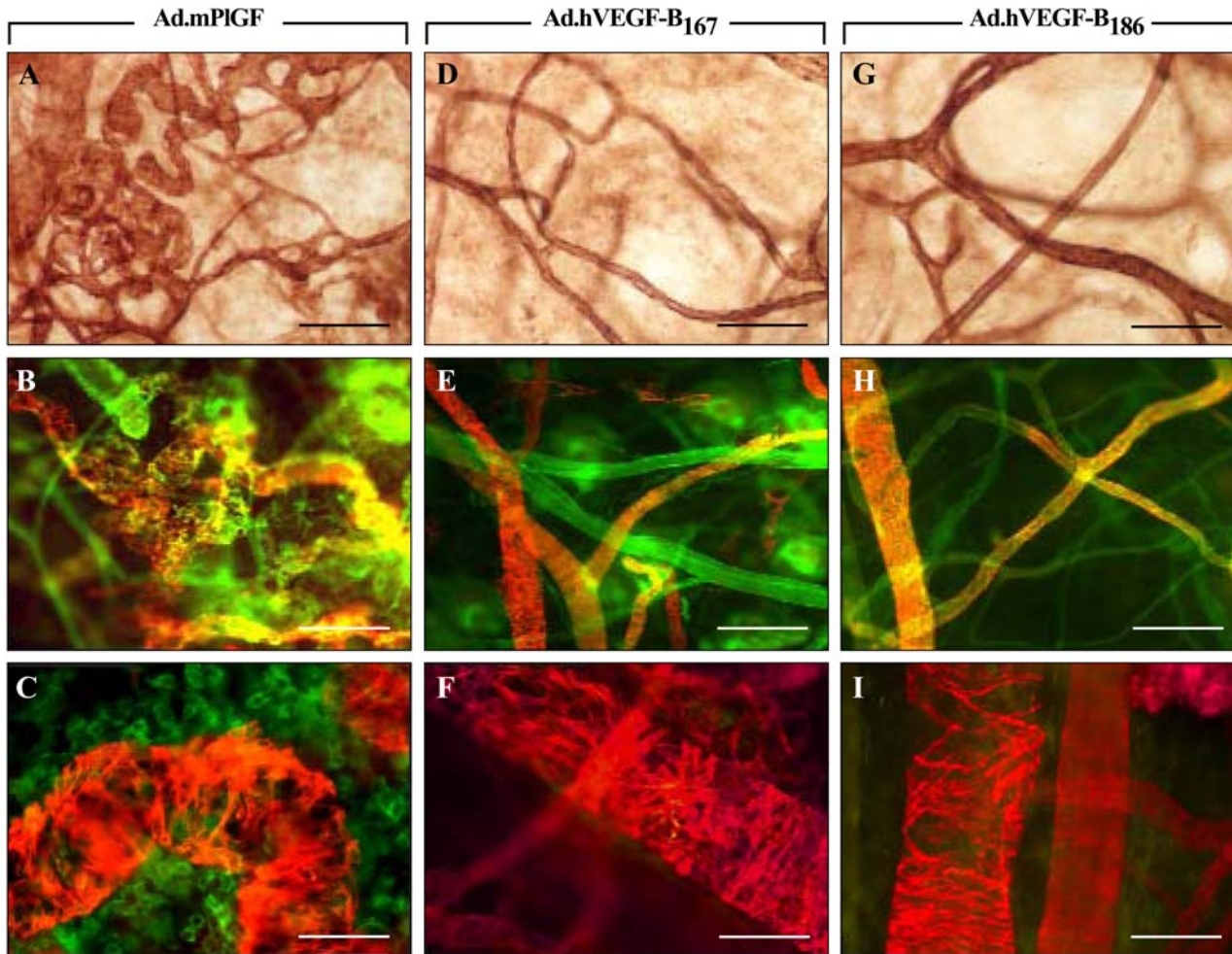
SUPPLEMENTAL REFERENCES

1. Leppanen P, Koota S, Kholova I, Koponen J, Fieber C, Eriksson U, Alitalo K, Yla-Herttuala S. Gene transfers of vascular endothelial growth factor-A, vascular endothelial growth factor-B, vascular endothelial growth factor-C, and vascular endothelial growth factor-D have no effects on atherosclerosis in hypercholesterolemic low-density lipoprotein-receptor/apolipoprotein B48-deficient mice. *Circulation.* 2005;112:1347-1352.
2. Li X, Aase K, Li H, von Euler G, Eriksson U. Isoform-specific expression of VEGF-B in normal tissues and tumors. *Growth Factors.* 2001;19:49-59.
3. Heymans S, Luttun A, Nuyens D, Theilmeier G, Creemers E, Moons L, Dyspersin GD, Cleutjens JP, Shipley M, Angellilo A, Levi M, Nube O, Baker A, Keshet E, Lupu F, Herbert JM, Smits JF, Shapiro SD, Baes M, Borgers M, Collen D, Daemen MJ, Carmeliet P. Inhibition of plasminogen activators or matrix metalloproteinases prevents cardiac rupture but impairs therapeutic angiogenesis and causes cardiac failure [see comments]. *Nat Med.* 1999;5:1135-1142.
4. Jang HS, Kim HJ, Kim JM, Lee YS, Kim KL, Kim JA, Lee JY, Suh W, Choi JH, Jeon ES, Byun J, Kim DK. A novel ex vivo angiogenesis assay based on electroporation-mediated delivery of naked plasmid DNA to skeletal muscle. *Mol Ther.* 2004;9:464-474.
5. Qian HS, Liu P, Huw LY, Orme A, Halks-Miller M, Hill SM, Jin F, Kretschmer P, Blasko E, Cashion L, Szymanski P, Vergona R, Harkins R, Yu J, Sessa WC, Dole WP, Rubanyi GM, Kauser K. Effective treatment of vascular endothelial growth factor refractory hindlimb ischemia by a mutant endothelial nitric oxide synthase gene. *Gene Ther.* 2006;13:1342-1350.
6. Springer ML, Chen AS, Kraft PE, Bednarski M, Blau HM. VEGF gene delivery to muscle: potential role for vasculogenesis in adults. *Mol Cell.* 1998;2:549-558.
7. Ozawa CR, Banfi A, Glazer NL, Thurston G, Springer ML, Kraft PE, McDonald DM, Blau HM. Microenvironmental VEGF concentration, not total dose, determines a threshold between normal and aberrant angiogenesis. *J Clin Invest.* 2004;113:516-527.
8. von Degenfeld G, Banfi A, Springer ML, Wagner RA, Jacobi J, Ozawa CR, Merchant MJ, Cooke JP, Blau HM. Microenvironmental VEGF distribution is critical for stable and functional vessel growth in ischemia. *Faseb J.* 2006;20:2657-2659.
9. Luttun A, Tjwa M, Moons L, Wu Y, Angelillo-Scherrer A, Liao F, Nagy JA, Hooper A, Priller J, De Klerck B, Compernolle V, Daci E, Bohlen P, Dewerchin M, Herbert JM, Fava R, Matthys P, Carmeliet G, Collen D, Dvorak HF, Hicklin DJ, Carmeliet P. Revascularization of ischemic tissues by PlGF treatment, and inhibition of tumor angiogenesis, arthritis and atherosclerosis by anti-Flt1. *Nat Med.* 2002;8:831-840.
10. Carmeliet P, Moons L, Luttun A, Vincenti V, Compernolle V, De Mol M, Wu Y, Bono F, Devy L, Beck H, Scholz D, Acker T, DiPalma T, Dewerchin M, Noel A, Stalmans I, Barra A, Blacher S, Vandendriessche T, Ponten A, Eriksson U, Plate KH, Foidart JM, Schaper W, Charnock-Jones DS, Hicklin DJ, Herbert JM, Collen D, Persico MG. Synergism between vascular endothelial growth factor and placental growth factor contributes to angiogenesis and plasma extravasation in pathological conditions. *Nat Med.* 2001;7:575-583.
11. Louzier V, Raffestin B, Leroux A, Branellec D, Caillaud JM, Levame M, Eddahibi S, Adnot S. Role of VEGF-B in the lung during development of chronic hypoxic pulmonary hypertension. *Am J Physiol Lung Cell Mol Physiol.* 2003;284:L926-L937.
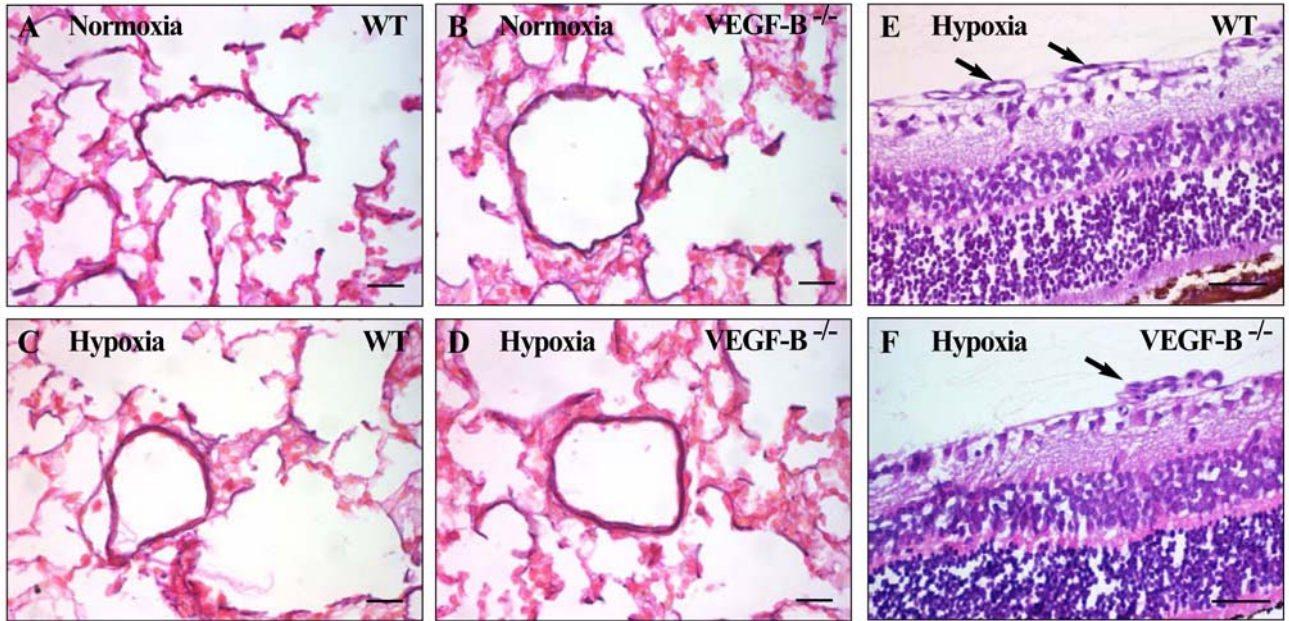
12. Reichelt M, Shi S, Hayes M, Kay G, Batch J, Gole GA, Browning J. Vascular endothelial growth factor-B and retinal vascular development in the mouse. *Clin Experiment Ophthalmol.* 2003;31:61-65.

13. Smith LE, Wesolowski E, McLellan A, Kostyk SK, D'Amato R, Sullivan R, D'Amore PA. Oxygen-induced retinopathy in the mouse. *Invest Ophthalmol Vis Sci.* 1994;35:101-111.

14. Brusselmans K, Compernolle V, Tjwa M, Wiesener MS, Maxwell PH, Collen D, Carmeliet P. Heterozygous deficiency of hypoxia-inducible factor-2alpha protects mice against pulmonary hypertension and right ventricular dysfunction during prolonged hypoxia. *J Clin Invest.* 2003;111:1519-1527.

15. Umans L, Cox L, Tjwa M, Bito V, Vermeire L, Laperre K, Sipido K, Moons L, Huylebroeck D, Zwijsen A. Inactivation of Smad5 in endothelial cells and smooth muscle cells demonstrates that Smad5 is required for cardiac homeostasis. *Am J Pathol.* 2007;170:1460-1472.

16. Banfi A, Springer ML, Blau HM. Myoblast-mediated gene transfer for therapeutic angiogenesis. *Methods Enzymol.* 2002;346:145-157.

17. Makinen T, Olofsson B, Karpanen T, Hellman U, Soker S, Klagsbrun M, Eriksson U, Alitalo K. Differential binding of vascular endothelial growth factor B splice and proteolytic isoforms to neuropilin-1. *Journal of Biological Chemistry.* 1999;274:21217-21222.
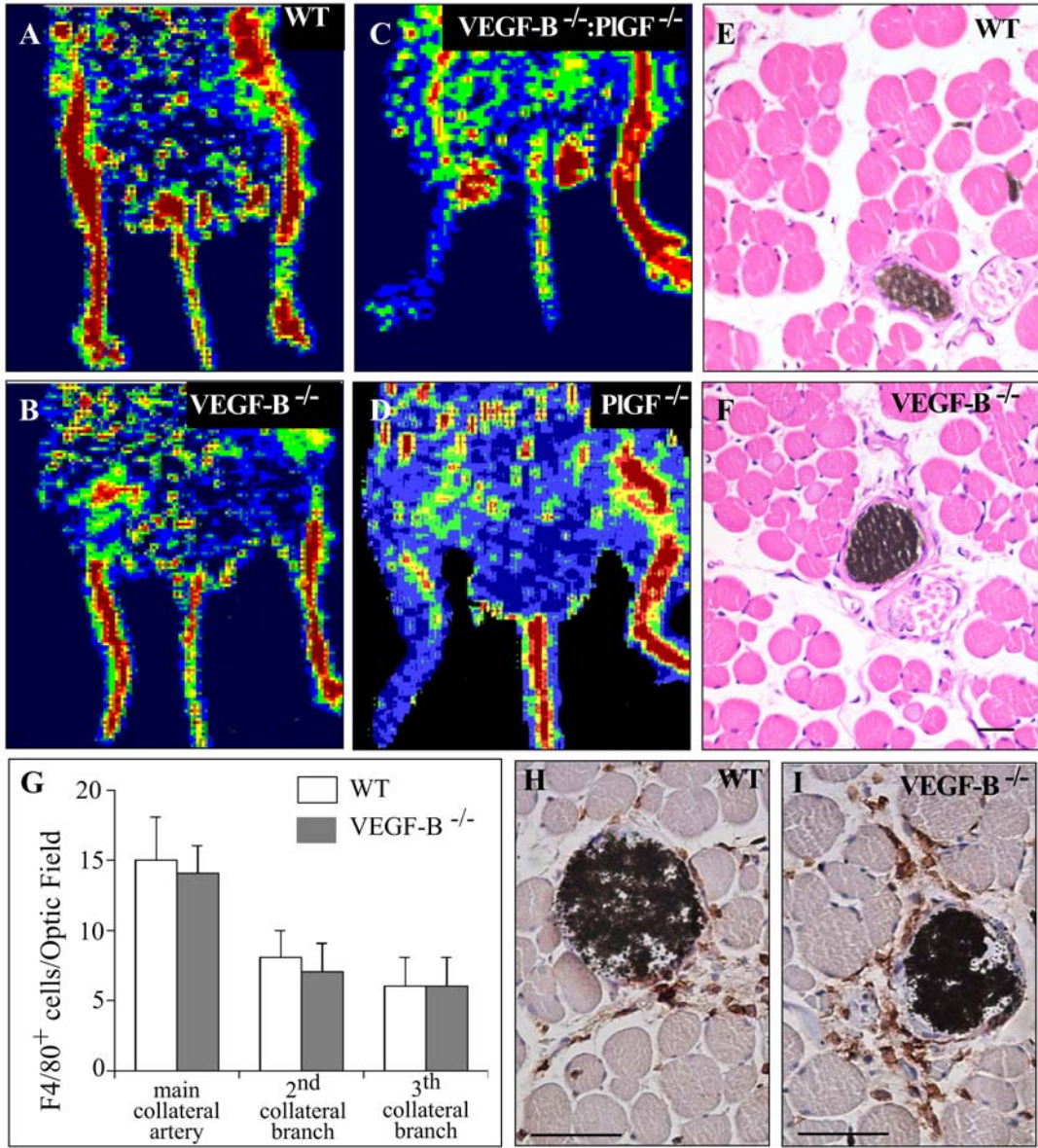
Supplement Figure ⎮

Ad.mPlGF   Ad.hVEGF-B$_{167}$ Ad.hVEGF-B$_{186}$

Supplement Figure II

Supplement Figure III

A   WT

C   VEGF-B $^{-/-}$:PlGF $^{-/-}$

E   WT

B   VEGF-B $^{-/-}$

D   PlGF $^{-/-}$

F   VEGF-B $^{-/-}$

G

H   WT

I   VEGF-B $^{-/-}$

Supplement Figure IV